Prediction of Molecular Weight Distributions Based on ab Initio Calculations: Application to the High Temperature Styrene Polymerization

Davide Moscatelli,*,† Carlo Cavallotti,*,† and Massimo Morbidelli‡

Dept. di Chimica, Materiali e Ingegneria Chimica "G. Natta", Politecnico di Milano, Via Mancinelli 7, 20131 Milano, Italy, and Swiss Federal Institute of Technology Zurich, Laboratorium für Technisdne Chemie/LTC, ETH-Höggerberg/HCI, CH-8093 Zurich, Switzerland

Received June 9, 2006; Revised Manuscript Received October 19, 2006

ABSTRACT: In this work we used quantum mechanics hybrid models (QM/QM) to investigate the high-temperature polymerization of styrene with the aim of elucidating its elementary chemistry. High and low quality quantum mechanics calculations were performed at the B3LYP/6-31g(d,p) and PM3 levels, respectively. Reaction kinetic constants were calculated for oligomers composed of up to 6 styrene units with classic transition state theory on potential energy surfaces determined at the QM/QM level. The capability of this approach to predict kinetic constants of elementary processes relevant to styrene polymerization was validated through the satisfactory comparison with well-known experimental data. One of the main results of this study is that a new kinetic route is proposed to describe the polymer growth mechanism, in which the succession of backbiting and β scission reactions plays a critical role. In particular we found that the 7:3 backbiting reaction can proceed fast and influence significantly the polymer weight distribution. Finally, the so evaluated kinetic constants were introduced in a polymerization reactor model and used to compare the distribution of the produced oligomers measured experimentally with that predicted from first principles. The agreement with experimental data is good, suggesting that the proposed approach provides a valuable tool to investigate the kinetics of polymerization systems for which experimental data on elementary reactions are not available.

1. Introduction

The high-temperature polymerization of styrene has been used for several decades in industry to produce large amounts of styrene oligomers, typically referred to as waxes. The kinetic mechanism responsible for styrene polymerization has been the subject of many investigations. First, the kinetics of the thermal initiation reaction was studied by Hui and Hamielec[1] and by Husain and Hamielec .[2] The developed models were able to simulate the monomer kinetics in the temperature range comprised between 100 and 230 °C, but they were less successful in predicting the oligomer molecular weight distribution. Successively, the same authors extended the model to predict the polymerization kinetics of styrene/acrylic acid copolymers in a CSTR up to 300 °C.[3] In order to refine these results, empirical relationship between molecular weight and both temperature and reactor residence time were introduced. The styrene polymerization kinetics was investigated at lower temperatures by Kirchner et al.[4] Several kinetic models have been developed to describe the polystyrene degradation mechanism, which were based on the introduction of a continuous molecular weight variable and on the use of kinetic mechanisms of increasing complexity.[5−8]

The styrene polymerization mechanism can be rationalized on the basis of these studies through the complex kinetic scheme shown in Figure 1. As for all free-radical polymerization systems, the kinetics is based on the classical chain mechanism involving initiation, propagation and termination steps. Because of the high temperatures considered in this study the mechanism is however more complicated. In addition to chain propagation (CP) reactions followed by combination (TA) or disproportionation (TD) termination reactions, dead polymer chains can be generated by two other mechanisms. The first consists in a random hydrogen abstraction reaction (RHA) of a radical on a dead chain followed by a β-scission reaction (left side of Figure 1), while the second is started by the transposition of the radical center from the chain end to an intermediate position, which can take place through a backbiting reaction (BB), followed by a β-scission reaction (β) (right side of Figure 1). For the sake of simplicity in this work, which is focused on oligomers, we do not consider branching reactions that can further complicate the reaction scheme. Thus, the main reaction events are the following:

$$S + S \xrightarrow{k_I} R_1^{\bullet} \tag{1}$$

$$R_m^{\bullet} + S \xrightarrow{k_{cp}} R_{m+1}^{\bullet} \tag{2}$$

$$P_n + R_m^{\bullet} \xrightarrow{k_{af}} R_{m+n}^{\text{mid-chain}\bullet} \tag{3}$$

$$R_m^{\bullet} \xrightarrow{k_{bb}} R_m^{\text{mid-chain}\bullet} \tag{4}$$

$$P_n + R_m^{\bullet} \xrightarrow{k_{ctp}} P_m + R_n^{\text{mid-chain}\bullet} \tag{5}$$

$$R_m^{\text{mid-chain}\bullet} \xrightarrow{k_{\beta}} P_n + R_{m-n}^{\bullet} \tag{6}$$

$$R_n^{\bullet} + R_m^{\bullet} \xrightarrow{k_{ta}} P_{m+n} \tag{7}$$

$$R_n^{\bullet} + R_m^{\bullet} \xrightarrow{k_{td}} P_m + P_n \tag{8}$$

* Corresponding authors. E-mail: carlo.cavallotti@polimi.it (C.C.); davide.moscatelli@polimi.it (D.M.). Telephone: ++39-02-23993176. Fax: ++39-02-23993180.

† Politecnico di Milano.

‡ Swiss Federal Institute of Technology Zurich.

10.1021/ma061291k CCC: $33.50 © 2006 American Chemical Society
Published on Web 12/19/2006

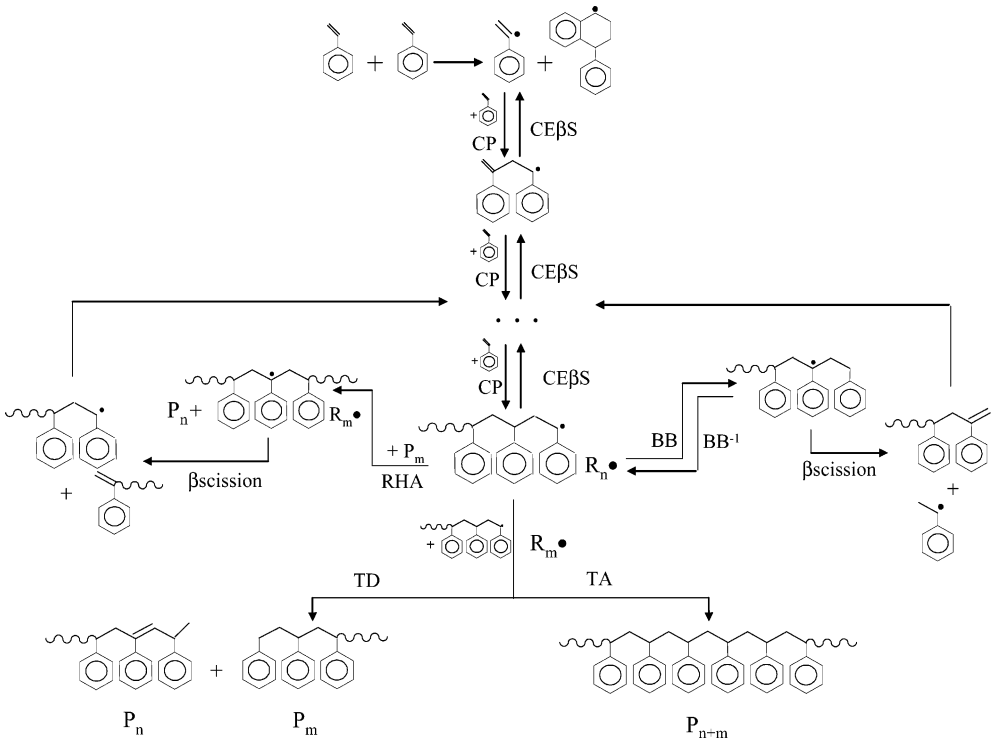

Figure 1. Global reaction mechanism of polystyrene production adopted in this work.

The self-initiating polymerization of styrene, represented by reaction 1, is conduced in a temperature range comprised between 250 and 350 °C. For this process, extended studies were performed to determine the complex initiation mechanism[9] and this will not be further analyzed in this work. The main effect of this reaction is that of producing the radicals which can then grow through the successive addition of styrene units (reaction 2, k_{cp}), or through addition fragmentation reactions (reaction 3, k_{af}), which are characterized by the formation of a midchain radical from a terminal-chain radical and a dead polymer. Addition fragmentation reactions, backbiting reactions (reaction 4, k_{bb}), which consist in an intramolecular hydrogen transposition in a radical, and chain transfer to polymer (reaction 5, k_{ctp}) reactions, in which a hydrogen is abstracted from a hydrocarbon chain by a free radical, lead to the production of free radicals with the unpaired electron positioned in the internal part of the polystyrene chain on a tertiary carbon atom. These radicals can give easily β-scission reactions (reactions 6, k_β), by which the carbon−carbon bond in the "β" position relative to the midchain radicals breaks forming a dead-chain and a free radical. Finally polymers can be produced by termination reactions, in which two radicals add to form a dead polymer (reaction 7, k_{ta}), or disproportionation termination reactions, in which a hydrogen tranfer between two radicals leads to the formation of two dead-chain polymers (k_{td}, reaction 8). The formation of a dead chain polymer can thus take place either through reactions 5−8.

The knowledge of the mechanisms of formation of polymer chains is of extreme importance in order to be able to tailor their properties. Thus, the first aim of this paper is to investigate the relative contribution of reactions 4−8 to the polymerization process. This is in fact a key step in the comprehension of the polymerization process, as the average polymer molecular weight is determined by the ratio of the rate of propagation to that of termination. The average degree of polymerization (D_n) can in fact be expressed as

$$D_n \propto \frac{k_p[M][R]}{k'_t[R]} = \frac{k_p[M]}{k'_t} \tag{9}$$

where k'_t represents the rate constant of the rate determining termination process. In particular k'_t is constant or proportional to [R] if the rate determining process is a unimolecular or bimolecular reaction, respectively.[10]

In order to identify the rate-determining step of the polymer termination process it is necessary to investigate in detail the kinetics of the degradation reactions. It has been recently proposed that the molecular weight distribution is not controlled by bimolecular termination reactions, and that the dominating termination process takes place through backbiting, leading to the formation of a midchain radical, followed by the production of dead-chain through a β-scission reaction. This conclusion was based mostly on fitting of experimental data simulated through reactor models using values of the relevant kinetic constants calculated with semiempirical methods.[10] Since recent NMR analyses have shown that branches are not formed in the high-temperature styrene polymerization,[11] the number of parallel reaction pathways active in this system is limited, which offers the possibility of performing a detailed kinetic analysis.

In this framework, the aim of this paper is to provide an accurate first principle estimation of the kinetic constants of the most important elementary reactions that take place during the styrene polymerization process. To pursue this aim, theoretical calculations were organized as follows. First a reliable ab initio calculation approach, based on our experience of modeling complex reacting systems, was chosen.[12−14] Then its capability to predict kinetic constants of elementary processes relevant to styrene polymerization was tested using as reference values well-known experimental data. Finally, the so evaluated kinetic constants were inserted into a polymerization reactor model. The aim is to compare the structure of the produced oligomers, mainly in terms of the chain length distribution measured experimentally, with the one predicted from first principles. This provides a hint on the contribution that first principle modeling

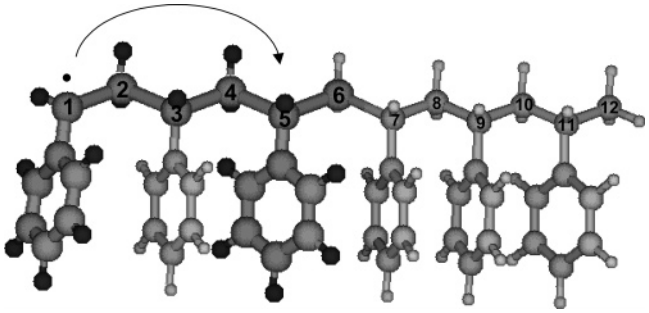

Figure 2. The 98 atoms model of polystyrene. The backbiting 1:5 reaction, where underlined atoms are those treated at a high level of theory, is reported schematically.

can give to the design of polymerization reactors, at least in the case of high-temperature styrene polymerization.

2. Computational Details

The styrene polymerization reactions investigated in this work are relatively simple molecular processes, as they involve the contemporary formation or cleavage of no more than two bonds. The difficulty arises from the large number of atoms that must be considered in each calculation, even if only small portions of the molecule are directly involved in the reaction. A computational approach that has been devised to treat such systems is a hybrid (QM/QM) approach, that allows to describe different parts of the same molecule at different levels of theory.[15−20] The hybrid computational method adopted is the ONIOM procedure, implemented in Morukama's group, that permits to subdivide a molecular system into different layers which can be described adopting different approaches (quantum mechanical, semiempirical, or molecular mechanics).[21,22] It is thus possible to treat the atoms more directly involved in the reaction using a suitable quantum mechanical method, while the remaining parts of the molecule, which role is often essentially steric, can be described at a much lower level of theory, using a semiempirical approach.

In this work all the QM/QM calculations were performed using the semiempirical PM3 method[23] to represent the part of the molecule farther from the reacting region and density functional theory (DFT) for the others.[24,25] In particular in all DFT calculations the exchange and correlation energy were calculated with the Becke 3 parameters and the Lee−Yang−Parr functionals.[26,27] The all electron 6-31 basis set with added polarization functions (6-31G-(d,p)) was used in the calculations.[28] All quantum chemical calculations of radicals were performed with a spin multiplicity of 2 and using an unrestricted wave function.

Six styrene units (98 atoms) composed the polystyrene molecular model chosen as representative of the polystyrene polymer. The assignment of the level of theory at which each atom is treated is an important choice, as it can influence significantly the outcome of the calculations. In the following, we refer to this assignment process as QM/QM or ONIOM partitioning. Our simulations, as will be discussed more in detail in the following, show that good results can be obtained if the primary chain of polystyrene and the benzene rings involved in the reactions are considered at the DFT level of theory, while the remainder is treated at the semiempirical level. The structure of the polystyrene model used to study the 1−5 backbiting reaction, where the parts of the molecule treated at the QM level of theory have been highlighted, is shown in Figure 2.

A second choice concerns the level of description of the stereochemical composition of the considered polystyrene chain. At the temperatures considered in this work free radical styrene polymerization produces an atactic polymer, characterized by a random relative orientation of the lateral phenyl groups. Though atactic polymers have different conformational properties with respect to isotactic or syndiotactic polymers, we expect stereochemistry to play a significant impact on the polymerization kinetics only for backbiting reactions. In fact propagation, termination, and

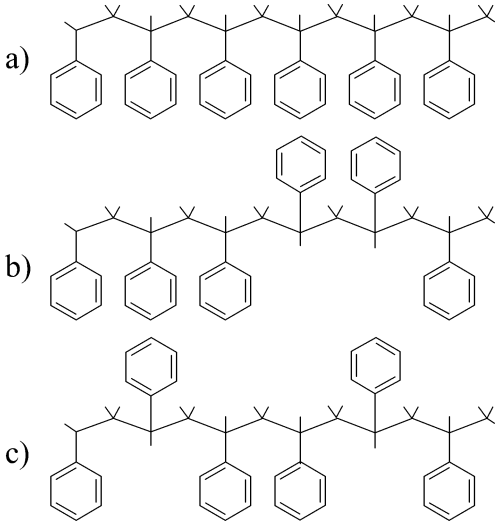

Figure 3. Structural models of polystyrene considered in the calculations: (a) isotactic, (b) SRRSS−R• atactic, and (c) SRSSR−R• atactic polymers.

β-scission reactions involve the formation or rupture of a single bond in a well-defined reacting zone, which involves few vicinal atoms. Moreover these reactions are not characterized by a significant distortion of the polymer main chain. This is however not the case for backbiting reactions, which involve the transfer of a hydrogen atom along the main polymer chain between sites that can be several angstroms distant. For this reason we have considered in this work three stereochemically different polystyrene molecular models, sketched in Figure 3, to represent the atactic polystyrene polymer kinetic behavior. The first is a six units isotactic polymer chain, while the others are two atactic chains with different relative orientation of the phenyl groups, to which we will refer to in the following as SRRSS−R• and SRSSR−R•. Kinetic constants were calculated using the following strategy. Propagation, termination, and β-scission reactions were determined only with the isotactic model, as no significant differences were expected for the other two models, while kinetic constants of all the considered backbiting reactions were determined using the three different molecular models.

In order to reduce the computational time necessary for geometry optimization, we first determined molecular structures and energies at the PM3 level, then the geometries so optimized were used as guesses for new geometry optimizations performed at the higher QM/QM level of theory. Several different structures were considered as starting point for the optimization process in order to improve the conformational search of the minimum energy structure. As a general rule, all geometries were fully optimized with the Berny algorithm and were followed by frequency calculations. A structure was considered stable only if possessing no imaginary vibrational frequencies.

The analysis of low vibrational frequencies of calculated minimum energy structures evidenced that many low vibrational frequencies are present. While some of them can be attributed to complex vibrational modes, other correspond to torsions around sp^3 bonds of the main polymer chain. The correct description of such motions would require the solution of the multidimensional Schrödinger equation for coupled rotors, an approach that is currently unfeasible given the complexity of the potential energy surface (PES) of this system (at least 10 dimensional, excluding the phenyl rotations). We therefore decided to calculate the partition functions associated with these torsions in the harmonic approximation. Though this approximation might seem restrictive, it must however be pointed out that relative internal motions in the structures here considered are significantly hindered by repulsive interactions between the phenyl groups, which are among the driving forces toward the formation of the 3^1 isotactic polystyrene helix. However, while such approximation is reasonable and can

Table 1. Comparison between Experimental and Calculated Rate Constant Values of the Propagation and Termination by Combination Reactions[a]

parameter	k_0 expt[33,34]	E_a expt[33,34] (kcal/mol)	k_0 calcd	E_a calcd (kcal/mol)
k_p	4.30×10^{10}	7.8	1.37×10^{10}	8.4
k_{tc}	1.06×10^{12}	1.5	1.13×10^{12}	0.0

[a] Geometries and frequencies were calculated by adopting the QM/QM method described in the text for the propagation constant and variational calculations for the termination by combination. Preexponential factors and activation energies are reported in units consistent with kcal, s, mol, and cm. The isotactic molecular model was used in the calculations.

be used as a reference value for future higher level treatments of internal rotations, it is known that in transition states torsional vibrations, because of the formation or cleavage of one or more bonds, can easily degenerate in relatively unhindered internal rotors. Since the corresponding partition functions can reach very high values, we decided to explicitly treat such motions, which we identified through vibrational frequency analysis, as uncoupled hindered rotors.[12,29]

Kinetic constants of reactions for which a distinct transition state could be identified were calculated with classic transition state theory. Transition state structures were located adopting the synchronous transit guided method[30] and are characterized by a single imaginary vibrational frequency. Activation energies were calculated as the difference between the electronic energy of the transition state and that of the reactant and include zero point energies (ZPE). For dissociation reactions proceeding without a distinct transition state kinetic constants were calculated with variational transition state theory (VTST). All quantum chemistry calculations were performed with the Gaussian 03 suite of programs,[31] while all pictures were drawn using Molden 4.2.[32]

3. Results and Discussion

The computational work was organized as follows. First we tested the QM/QM computational approach calculating the kinetic constants of well-known reactions related to the reacting system under examination. Then we calculated the kinetic constants of key reactions involved in the polymerization process, thus developing a framework for compiling a kinetic mechanism consisting of elementary reactions. Finally we embedded the detailed kinetic mechanism in a continuous stirred tank reactor (CSTR) model and simulated experimental data collected in previous works.[10] This allowed as to draw some conclusions on the main kinetic pathway determining the high-temperature polystyrene polymerization process. Three different detailed kinetic mechanisms, corresponding to three stereochemically different molecular models, were considered in the calculations. In the following we mostly report the CSTR simulation results determined using the isotactic molecular model, as they are intermediate between those obtained with the other two models, which are however reported as Supporting Information.

3.1. Method Validation. As a first part of this work, we tested the capability of our computational approach to evaluate kinetic constants of relevant reactions involving styrene for which experimental data are available. This operation has required to individuate a set of reactions whose kinetic constants have been measured at a high level of accuracy. This is indeed the case for the propagation kinetic constant, reaction 2, as well as for the termination kinetic constant, reaction 7, reported by Buback et al.[33,34] Both kinetics have been studied through pulsed-laser polymerization (PLP) in conjunction with molecular weight distribution and styrene conversion measurements. The measured kinetic constants are reported in Table 1.

A. Calculation of the Propagation Kinetic Constant. The kinetic constant of monomer addition was calculated using the polystyrene molecular model sketched in Figure 2 and the computational approach described in section 2. In order to determine the ONIOM partitioning of the model molecule that gives best agreement with the experimental data, four different cases have been considered. Two calculations were performed in which all atoms were treated in one case with a semiempirical approach (PM3) level and in the other using density functional theory (B3LYP/6-31g(d,p)). The latter represents our reference system and ideally is the one best suited to investigate a complex reacting system. However it is computationally onerous, and therefore, we decided to treat some part of the model molecule at a lower level of theory. Two different systems were considered. In the first case, only the main polystyrene chain was treated at a high level of theory and the other atoms at a lower one; in the second, both the main polystyrene chain and the benzene rings involved in the reaction are considered at the high level of theory. The benzene rings involved in the reaction are two and are those bonded with the reacting tertiary radical-carbon atoms, as shown in Figure 2. In the second case, the explicit consideration of the benzene rings at the DFT level has the purpose of improving the description of the hyperconiugation effect of tertiary carbon atoms bonded to aromatic units, which is unlikely to be correctly described by a semiempirical approach.

Reactant and transition state structures and energies were determined for the four investigated molecular models. The calculated propagation activation energies, as well as some key geometrical parameters are reported in Table 2, while the transition state structure is sketched in Figure 4. As it can be observed, the activation energy calculated adopting the QM/QM partitioning in which only the main polystyrene chain is treated at the high level of theory differs only by 0.3 kcal/mol from that calculated using DFT for all the atoms, while that determined at the PM3 level differs by about 3 kcal/mol. Interestingly the activation energy computed considering the main polystyrene and the benzene rings involved in the reaction at the high level of theory is equal to the reference value. Thus, we decided to perform all the following calculations using this QM/QM partitioning of the molecular model. Finally it is important to observe that the difference between calculated and experimental activation energy, as shown in Table 1, is less than 1 kcal/mol (0.6 kcal/mol), which shows that DFT calculations performed at the B3LYP/6-31g(d,p) level can describe very well polystyrene reactions, at least for the investigated case.

The calculation of the pre-exponential factor for the polystyrene chain propagation reaction is complicated by the fact that this polymer has several internal rotational degrees of freedom. The frequency analysis of the transition state structure has in fact shown that three vibrational frequencies smaller than 150 cm^{-1} can be attributed to internal rotations. The low vibrational frequencies are 47.47, 70.94, and 93.50 cm^{-1} and correspond to the internal motions shown in Figure 5. The degeneration of a vibrational in a rotational motion can significantly affect the calculation of a pre-exponential factor of a bimolecular reaction since a rotational partition function is usually significantly larger than a vibrational one. These internal motions were treated as hindered rotors. The corresponding partition functions were calculated using the method proposed by Fascella et al.[12] This requires to calculate the potential energy surface for the rotation of a part of the molecule with respect to the other, which was performed using the ONIOM method

Table 2. Comparison of Activation Energies of the Propagation Reaction (k_p) Calculated Adopting Different QM/QM Partitioning and the Isotactic Molecular Model

QM/QM partitioning	E_a calcd (kcal/mol)	d_1	d_2	d_3	a_1	a_2
all PM3	11.0	1.43	1.38	2.15	122.9	106.0
all DFT	8.3	1.46	1.38	2.26	126.8	109.9
QM(DFT main chain)/QM	8.7	1.43	1.45	1.97	126.1	111.4
QM(DFT main chain + involved styrene)/QM	8.4	1.46	1.38	2.27	126.6	109.9

Table 3. Comparison between Vibrational (Q_{vib}^{int}) and Internal Rotation (Q_{rot}^{int}) Partition Functions for Three Significant Low Vibrational Frequencies (Isotactic Molecular Model)

associated rotation	ν [cm^{-1}]	Q_{vib}^{int}	Q_{rot}^{int}
r_1	47.47	4.91	7.18
r_2	70.94	3.465	7.33
r_3	90.50	2.77	14.51

Table 4. Calculated Partition Functions, Molecular Energies (the Reference Is the Reactant) and Kinetic Constant for Different Reaction Coordinate (d) Values for the Termination by Combination Reaction (Isotactic Molecular Model)

D (Å)	E_a(d) (kcal/mol)	Q_{rot1}^{2}D	Q_{rot2}^{2}D	Q_{rot}^{1}D	$Q_{rot}^{\neq}$tot
4.5	39.9	675.6	13 690	113.21	2.28×10^{11}
5.0	42.2	670.1	13 690	113.21	2.30×10^{11}
5.5	44.0	661.8	13 690	113.21	2.33×10^{11}
6.0	45.0	653.3	13 690	113.21	2.38×10^{11}
6.5	46.1	615.9	14 975	113.21	2.48×10^{11}
7.0	46.9	722.1	15 610	113.21	2.88×10^{11}
7.5	47.8	2684.6	37 594	113.21	2.95×10^{11}

described above. The calculated rotational PES for the R_1, R_2, and R_3 motions are shown in Figure 6. Subsequently the PES was interpolated using cubic splines and the internal rotation partition function was evaluated as

$$Q_{rot,int} = \frac{1}{\sigma_{int}} \sum_k g_k \exp\left(-\frac{\epsilon_k}{k_B T}\right) \tag{10}$$

where g_k is the degeneracy of the rotational energy level ϵ_k and σ_{int} is the symmetry number of the internal rotation; g_k, ϵ_k, and σ_{int} are determined by solving a one-dimensional Schrödinger equation.[13]

The maximum energetic barrier for the R_1 internal rotation is 13.0 kcal/mol, as shown in Figure 6. Similar results are obtained with other two low vibrational frequency which correspond to the rotational motion around the polystyrene-($CH-C_6H_5$) bond and the polystyrene-($CH_2-CH-C_6H_5$) bond, respectively. The calculated internal partition functions are compared with the corresponding vibrational partition functions in Table 3 and were used to evaluate the pre-exponential factor of the investigated reaction through transition state theory. As it can be observed, the explicit consideration of internal motions as hindered rotors led to an increase by a factor of 10 the kinetic constant. The calculated pre-exponential factor of 6.65×10^{10} is in good agreement with the experimental value of 4.3×10^{10}.

B. Calculation of the Termination by Combination Kinetic Constant. Termination by combination is a family of exothermic reactions characterized by the formation of a single σ bond between two reacting radicals. These reactions usually proceed without passing through a distinct transition state, which makes classic transitional theory inapplicable. In these cases, it is possible to evaluate an upper limit of the kinetic constant using variational transition state theory (VTST). In its essential features, VTST requires to scan the reaction PES and to evaluate the reaction kinetic constant using TST as a function of the reaction coordinate. The VTST kinetic constant value is the minimal of those calculated through this procedure. For the low viscosity values characteristic of the high-temperature styrene polymerization, it is reasonable to assume that the reaction kinetics is independent of the length of the polymeric chain. We therefore choose as molecular model of the reactants two identical molecules, each one comprising two monomeric units. Thus, the reaction can be written as

$$R_2 + R_2 \xrightarrow{k_{ta}} P_4 \tag{11}$$

Calculations were performed using the QM/QM partitioning procedure introduced in the previous section that gave results in good agreement with those obtained with a full calculation using DFT level.

The measured experimental activation energy for this process is very low, 1.5 kcal/mol. Even if this might suggest the existence of a transition state, our analysis, performed by both scanning the PES as a function of the length of the bond that is being formed and using an automatic algorithm for the search of a saddle point,[30] could not find a maximum on the PES. In particular, we calculated that the reaction is exothermic by 49.5 kcal/mol, which is in agreement with the 47.8 ± 1.5 suggested value for this class of bonds.[35] Our calculations have also shown that the total energy of the investigated system increases constantly with the length of the bond that is being broken. To determine the kinetic constant of the termination reaction we followed a reverse approach. We first evaluated the kinetic constant of the inverse reaction, the dissociation of P_4 in R_2, and then determined k_{ta} by applying thermodynamic consistence (i.e., from the equilibrium constant) with calculated enthalpy and entropy changes. The calculated entropy change for the dissociation reaction is 43.8 (cal/K)/mol. When applying VTST, it is important to explicitly consider the possibility that some internal vibrations degenerate in hindered internal rotors. To account for this, we calculated the VTST kinetic constant using the following equation:

$$K_{cin}^{backward} = \frac{k_B T}{h} \cdot \frac{Q_{tot}^{\neq}}{\prod_{reactants} Q_{rot}^{i} \cdot Q_{vib}^{i} \cdot Q_{el}^{i}} e^{(\Delta(E_0(d)+ZPE)/(RT)} \tag{12}$$

where $E_0(d)$ is the difference between the electronic energy of the reacting molecule calculated when the length of the bond that is being broken is d. The molecular partition function of the transition state $Q^{\neq}$ was calculated following the procedure suggested by Gilbert[36] as

$$Q_{tot}^{\neq} = Q_{vib}^{R_2} \cdot Q_{vib}^{R_2} \cdot Q_{rot}^{\neq tot} \cdot Q_{rot1}^{2D} \cdot Q_{rot2}^{2D} \cdot Q_{rot}^{1D} \tag{13}$$

$$Q_{rot}^{1D} = \left(\frac{\pi k_B T}{\sigma^2 B}\right)^{1/2} \quad Q_{rot}^{2D} = \left(\frac{k_B T}{B}\right) \tag{14}$$

where Q_{vib}^{R2} is the vibrational partition function of R2, $Q_{rot}^{\neq tot}$ is the external rotational partition function of the reacting molecule, Q_{rot1}^{2D} and Q_{rot2}^{2D} are the internal rotational partition functions of the 2D rocking motions of the two moieties in which the reactant

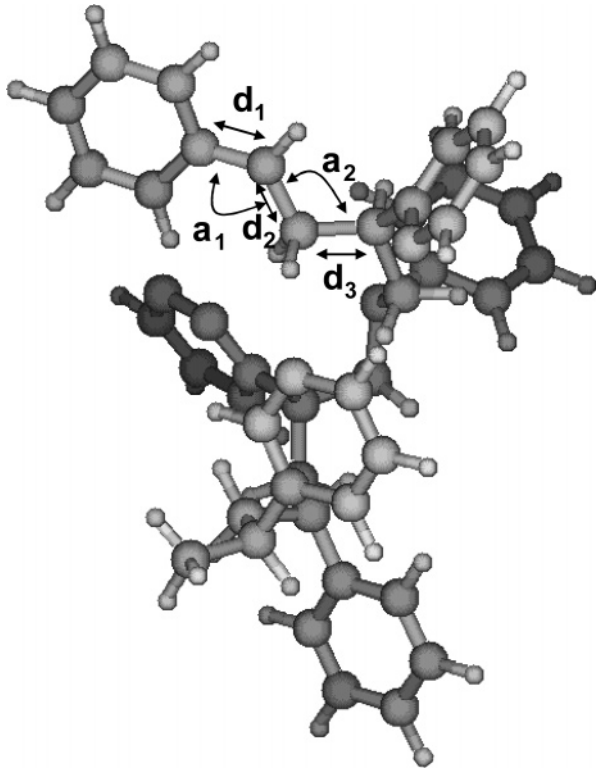

Figure 4. Transition state structure of the propagation reaction (isotactic molecular model).

is being dissociated, Q_{rot}^{1D} is the 1D partion function for the torsional mutual rotation of the two moieties around the breaking bond, B is equal to $(h^2/8)\pi^2 I$, and σ is the rotational symmetry number. The reduced moments of inertia for all the internal rotations, as well as hindrance angles that can limit these relative motions, were calculated using the GEOM program distributed with the UNIMOL suite.[37]

According to the VTST described above, the kinetic constant depends on two factors: the reaction activation energy and the pre-exponential factor. Both of them are function of the reaction coordinate and increase with it. The calculated partition functions, molecular energies and kinetic constants are reported in Table 4 for different reaction coordinate values at a temperature of 600 K.

Next the kinetic constant was interpolated and its minimum value was found at a distance of 6.84 Å, which we thus considered as the transition state. The calculated activation energy and pre-exponential factor are 46.7 kcal/mol and 5.0×10^{11} s^{-1}. Then the termination by combination rate constant was calculated from thermodynamic consistence, and was found to be 1.1×10^{12} at 300 K and 4.3×10^{11} $cm^3/mol \cdot s$ at 600 K, which is near the experimental value of 3.1×10^{11}, measured at 600 K.

The experimental and calculated data for the reactions investigated in this section are summarized in Table 1.

3.2. Dominant Chain Growth Mechanism. The dominant chain growth mechanism investigated is sketched in Scheme 1, where the possible reactions of a R_n radical are summarized. A growing radical R_n can depolymerize to give a R_{n-1} radical, add a monomer to form R_{n+1}, or isomerize through a backbiting reaction transposing a hydrogen atom to form a mid chain radical. As sketched in Figure 2, the hydrogen atoms that are statistically more likely to give backbiting reactions are those attached to the tertiary carbon atoms in positions 3, 5, and 7. Once formed, the mid chain radical can follow two different

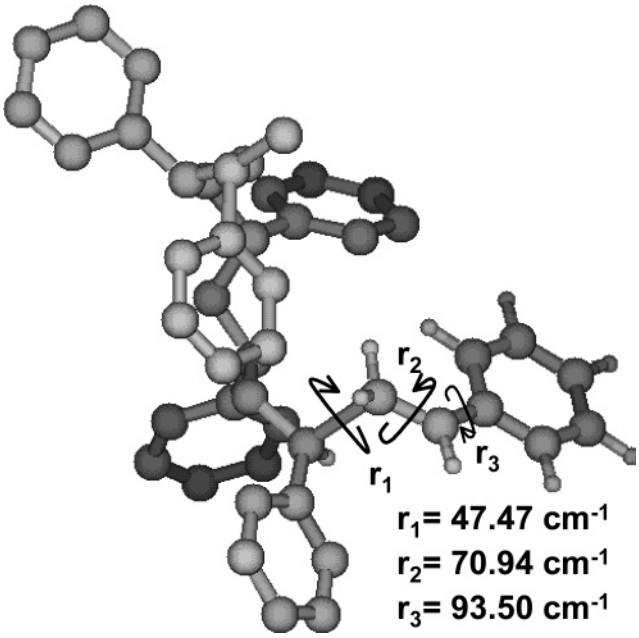

Figure 5. Assignment of the three vibrational frequencies treated as free internal rotors (isotactic molecular model).

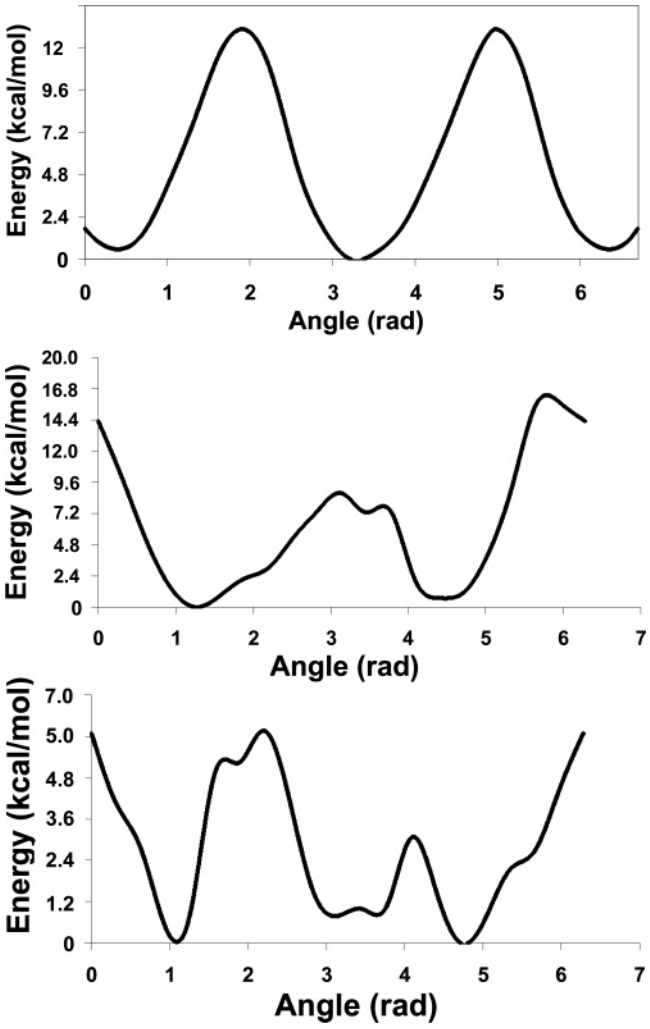

Figure 6. Rotational potential energy for the three internal rotors of the transition state for the propagation reaction described in the text (isotactic molecular model).

reaction pathways: decompose through a β-scission reaction into an oligomer (P) and another radical (R′), or transpose back

Scheme 1. Possible Reactions of a Midchain Radical

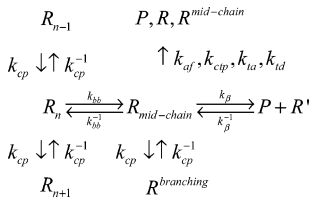

the hydrogen forming again the R_n terminal radical. This represents a pathway for the production of oligomers that is in competition with bimolecular terminations. While for the latter good kinetic constants estimates are available, this is not the case for the backbiting and β-scission mechanism. For this reason we decided to investigate in detail this last reaction pathway.

A. Backbiting. Hydrogen transposition in a R_n terminal radical can easily occur at the process temperature because of the high reactivity of the radical in the terminal position of the growing chain. In particular the abstraction of a hydrogen atom bonded with a tertiary alkyl carbon is more favorite with respect to other hydrogen atoms, because it leads to the formation of a tertiary radical, which is the most stable carbon radical. Sterically and energetically, the third, fifth, and seventh tertiary carbons from the chain-end are the more favorable positions for hydrogen transposition.[10]

The backbiting reactions of 1:3, 1:5, and 1:7 hydrogen transposition, reported in Scheme 2, were investigated adopting the QM/QM partitioning procedure previously described. All reactions are slightly exothermic, and in particular by 1.1, 0.3, and 1.2 kcal/mol for the 1:3, 1:5, and 1:7 transposition, respectively, for the isotactic polymer. The kinetic constants calculated for the three considered structural models (isotactic and atactic, as reported in Figure 3) were determined with transition state theory and are reported in Table 5 (where we also reported the kinetic constant for the 7:3 backbiting reaction, which relevance to styrene polymerization is described in paragraph 3.3), while the corresponding transition state structures are shown in Figure 7 for the isotactic model.

The calculated activation energies for the isotactic chain are 41.3, 17.9, and 21.7 kcal/mol, respectively. As can be observed, the 1:5 hydrogen transposition is the most favorite, while the 1:3 reaction requires overcoming a high-energy barrier. These results may be explained in terms of transition state stability. In fact, the 1:5 backbiting reaction leads to the formation of a 6 membered ring transition state characterized by a low internal strain, while the 1:3 backbiting reaction is much less favorite because its transition state is a highly strained 4 membered ring. To test the correctness of this interpretation we studied at the B3LYP/6-31g(d,p) level the same backbiting reactions, but in the case of polyethylene. This allows one to eliminate the effect of steric hindrances and mutual repulsions due to the phenyl rings of polystyrene. The calculated activation energies for this process were 38.7, 18.3, and 18.4 kcal/mol for 1:3, 1:5, and 1:7 backbiting, respectively, for the isotactic polymer. This confirms our hypothesis that the difference in activation energies for the three reactions is due to the strain of the main polymeric chain in the transition state rather than to interactions among the styrenic rings. Once formed, midchain radicals can then react following the different pathways shown in Scheme 1.

Activation energies and enthalpy changes calculated for the two atactic chains are similar to those obtained for the isotactic polymer, with reactions rates generally slightly slower. This can be attributed to repulsive intramolecular interactions between the phenyl rings in the transition state, with respect to those found for the isotactic chain, which presents a well-defined 3_1-helix structure.

It is interesting to compare the backbiting reaction rates reported in Table 5 with those proposed in the literature for H internal transfer in linear alkane radicals.[38,39] These works propose that pre-exponential factors decrease substantially with the number of atoms in the transition state ring structure. This trend can be ascribed to the blocking of internal rotations in the transition state. On the contrary, the data reported in Table 5 do not show any significant variation in pre-exponential factors. This is due to the fact that we treated torsional motions around the main polystyrene chain in the harmonic approximation, rather then as free or hindered rotors. Thus, the negligible dependence of pre-exponential factors from the transition state ring size can be ascribed to the low sensitivity of vibrational frequencies to the structural deformation necessary to reach the transition state. In order to check whether this approximation is reasonable, partition functions of transition state and reactant might be computed considering the internal rotations along the main polymer chain as a system of hindered coupled rotors. As discussed in the method section, this is a task particularly complicated by the high dimensionality of the PES to be considered, and is likely to give results significantly different from those proposed for linear alkane radicals. While in fact internal rotations in alkanes are only slightly hindered, this is not the case for polystyrene, because of the repulsive interactions among phenyl groups and partial sp^2 hybridization of the radical center.

B. β-Scission. This is a unimolecular decomposition reaction of a mid chain radical that involves the rupture of a C−C σ bond between a secondary and a tertiary carbon atom partially compensated by the formation of a π bond. The reaction is symmetric since the mid chain radical can react to form the π bond with the secondary carbon atoms positioned at its immediate left or right.

The products of this reaction can be several, as shown in Scheme 3. Following the β-scission reaction a midchain radical, composed by (n) monomers and produced as a result of a 1:5 backbiting reaction, can, for example, form either the 2,4,6-triphenyl-1-exene and a ($n - 3$) units terminal chain radical (β15) or a dimer radical and an unsaturated dead chain formed by ($n - 2$) styrene monomers. β-scission reaction from a mid-radical in position 7 produces both the 2,4,6,8-tetra-phenyl-1-octene and a ($n - 4$) units terminal chain radical, or a trimer radical and an unsaturated polymer formed by ($n - 3$) units. β-scission from a mid-radical in position 3 produces both 2,4-diphenyl-1-butene and a ($n - 2$) units radical molecule, or ($n - 1$) polymer units chain and a benzylic radical. Finally, a β-scission from a radical in position 1 is equal to a depropagation reaction to form styrene and the relative growing radical.

The first reaction investigated has been that of depropagation. Adopting the ONIOM partitioning introduced above, transition state theory, and the isotactic molecular model it was found that this reaction requires an activation energy of 19.6 kcal/mol with a pre-exponential factor of 1.7×10^{12} s^{-1}. Moreover we calculated that both the right and left β-scission reactions have the same activation energy, while the activation energy changes with the position of the midchain radical. The transition state geometry for the β-scission reaction of the polystyrene mid chain radical in position 5 is shown in Figure 8. It is interesting to observe that the distance between the carbon atoms in position 6 and 7 is smaller than that between the carbon atoms in position 7 and 8. This is due to the change of the ibridation state from sp^3 to sp^2 of the carbon atom in position 6, which

Scheme 2. Backbiting Reactions

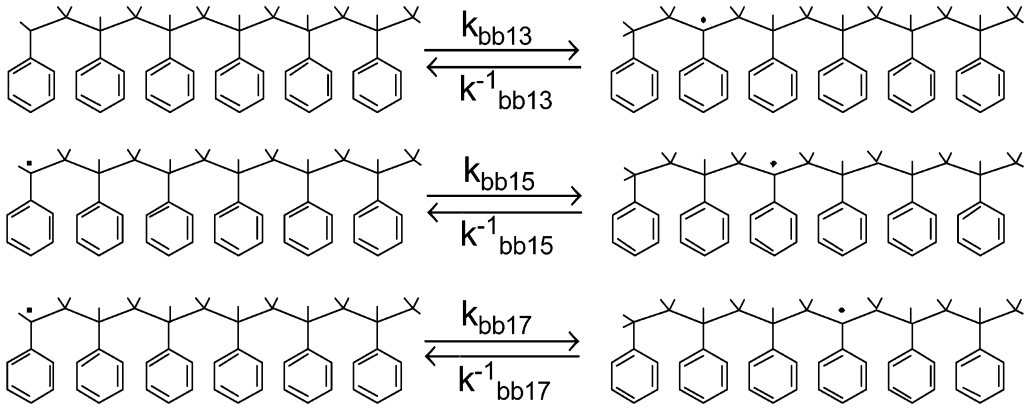

Table 5. Calculated Rate Constants for Backbiting Reactions for the Three Different Molecular Models Considered in This Work[a]

reaction		$\log_{10} A$	E_a		$\log_{10} A$	E_a
		Isotactic Model				
$R_{n,1} \rightleftarrows R_{n,3}$	k_{bb13}	11.340	41.30	k_{bb13}^{-1}	11.834	42.50
$R_{n,1} \rightleftarrows R_{n,5}$	k_{bb15}	10.773	17.92	k_{bb15}^{-1}	11.447	18.10
$R_{n,1} \rightleftarrows R_{n,7}$	k_{bb17}	11.620	21.70	k_{bb17}^{-1}	12.046	23.50
$R_{n,7} \rightleftarrows R_{n,3}$	k_{bb73}	11.372	16.90	k_{bb73}^{-1}	11.362	18.13
		RRRSS−R• Atactic Model				
$R_{n,1} \rightleftarrows R_{n,3}$	k_{bb13}	11.516	41.05	k_{bb13}^{-1}	12.053	43.39
$R_{n,1} \rightleftarrows R_{n,5}$	k_{bb15}	11.102	21.96	k_{bb15}^{-1}	11.118	22.00
$R_{n,1} \rightleftarrows R_{n,7}$	k_{bb17}	10.839	20.48	k_{bb17}^{-1}	10.440	22.34
$R_{n,7} \rightleftarrows R_{n,3}$	k_{bb73}	10.944	22.82	k_{bb73}^{-1}	11.241	23.76
		RSRRS−R• Atactic Model				
$R_{n,1} \rightleftarrows R_{n,3}$	k_{bb13}	11.757	44.30	k_{bb13}^{-1}	11.973	44.31
$R_{n,1} \rightleftarrows R_{n,5}$	k_{bb15}	11.360	18.81	k_{bb15}^{-1}	11.614	19.65
$R_{n,1} \rightleftarrows R_{n,7}$	k_{bb17}	10.707	20.54	k_{bb17}^{-1}	9.795	22.40
$R_{n,7} \rightleftarrows R_{n,3}$	k_{bb73}	11.431	20.30	k_{bb73}^{-1}	12.253	23.57

[a] Pre-exponential factors and activation energies reported in units consistent with kcal, s, mol, and cm as $k = A \exp(-E_a/RT)$.

results in the formation of the terminal double bond that characterizes the oligomer.

The calculated kinetic constants for the β-scission of mid chain radicals in positions 3, 5, and 7 are reported in Table 6. Computed activation energies are comprised between 20.0 and 24.2 kcal/mol while pre-exponential factors are almost the same.

3.3. Reactor Simulations and Data Analysis. In order to identify the dominant chain growth mechanism, it is necessary to perform a simulation of the polymerization process in which all the relevant involved reactions are explicitly considered. For this purpose, the reaction rates calculated in the previous section were embedded in a kinetic scheme and inserted in a perfectly stirred reactor model to simulate the experimental setup described in ref 10. The range of temperatures and residence times investigated is comprised between 250 and 350 °C and 5 and 90 min, respectively. The reaction scheme is composed of 68 chemical species involved in 378 reactions, which describe step by step the conversion of the styrene monomer in an oligomer composed of up to 16 monomers. The reaction scheme is summarized in Tables 5 and 6 and includes: the initiation reaction, polymerization and depolymerization reactions; 1:3, 1:5, 1:7, and 7:3 forward and backward backbiting reactions; β-scission reactions, and all the possible radical combination and disproportionation termination reactions. We considered three different kinetic schemes, corresponding to the three molecular models adopted to describe the random configuration of the polystyrene oligomer. The kinetic schemes differ for the rates of the backbiting reactions. All simulations were repeated for the three different sets of reactions, though we mostly report here the results obtained with the isotactic kinetic scheme, as they are intermediate between those obtained using the atactic models. However, the calculated results are qualitatively similar and differ only slightly quantitatively, as can be observed by comparing the polymer weight distribution obtained for 90 min residence time at 343 °C, reported in Figure 9, for the three different structural models considered. Therefore, in order to limit the discussion, we decided to comment in detail in the following only the results obtained with the isotactic scheme, while we report as Supporting Information the data calculated with the two other kinetic schemes.

It is worth noting that with respect to the lumped kinetic model developed by Campbell et al.,[40] we have included here the new backbiting reaction 7:3 as well as the reversibility of all backbiting reactions, i.e., the backward backbiting reactions 7:1, 5:1, 3:1, and 3:7. This was suggested by the results of the QM calculations discussed in section 2, which showed that the activation energy for backward reactions is relatively small. Similarly the 7:3 backbiting reaction has been introduced because, passing through an unstrained six-membered ring transition state, has a low activation energy.

The results of the simulations performed with a residence time of 90 min are reported in Figure 10a for four temperatures: 260, 288, 316, and 343 °C, in terms of the molecular weight distribution. We found that the oligomer weight distribution is rather broad at the lowest temperature, while it moves toward smaller molecular weights as the temperature increases, and it is in fact centered on dimers and trimers at the highest temperature. This is in good agreement with the experimental data shown in Figure 10b.[10] At the lower temperatures the molecular weight distributions show a peak in proximity of the trimer and are centered over molecular weight up to 1000 Da. Simulations at higher temperatures are centered about smaller oligomers and maintain the same trend as a function of temperature as shown by the experimental results. The only significant disagreement between experimental and calculated data is at the highest temperatures, i.e., 343 °C, where the simulations overpredict the dimers production. We will come later to discuss this point in detail, while we now proceed to analyze the effect of the residence time in the reactor.

The results of simulations performed at 316 °C and for residence times ranging from 5 to 90 min are shown in Figure 11a. It can be observed that the effect of temperature and residence time is similar. This is particularly true for low molecular weight oligomers, with dimers and trimers being the must abundant species for higher residence times. The simulations are in agreement with the experimental data shown in

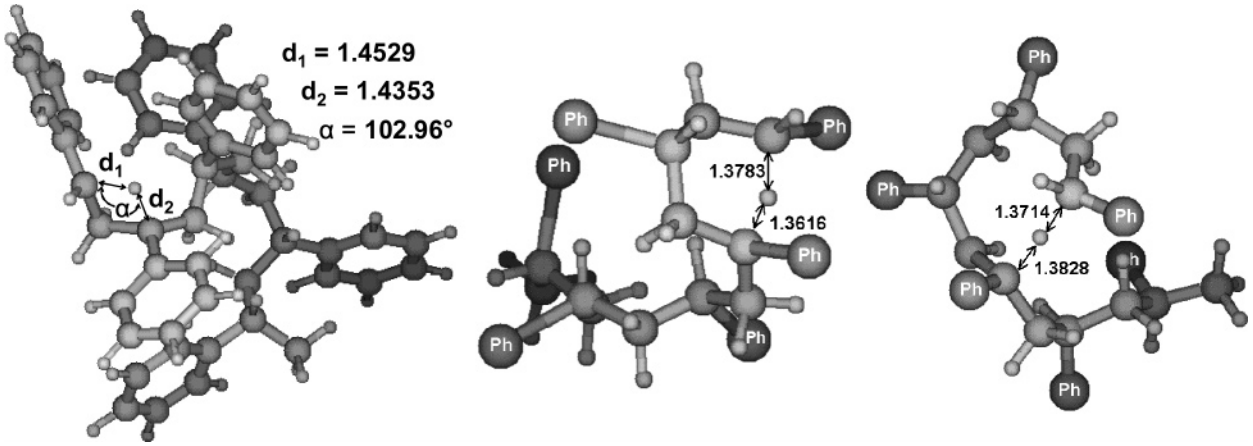

Figure 7. Transition state geometry for the polystyrene 1:3, 1:5 and 1:7 backbiting reactions calculated with QM/QM ONIOM partitioning. Distances are reported in angstroms and angles in degrees (isotactic molecular model).

Scheme 3. *β*-Scission Reactions

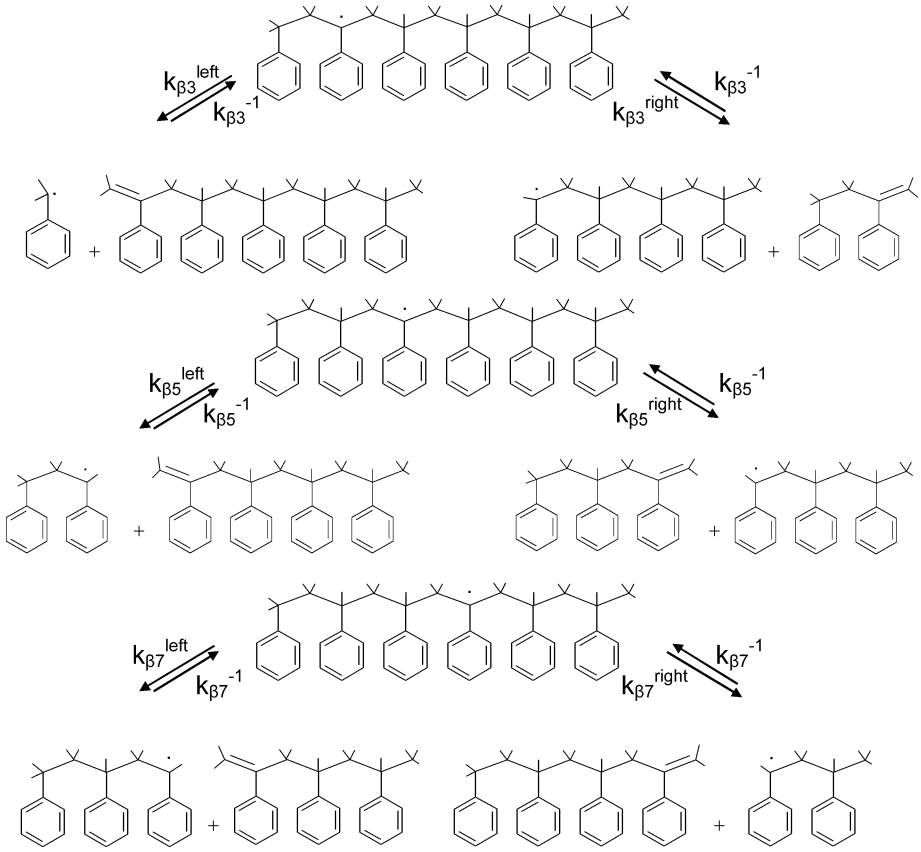

Figure 11b.[10] In particular it is seen that the dimer, trimer, and tetramer concentrations increase with residence time as is also observed experimentally. It can be noted that the production of high molecular weight oligomers seems to be more influenced by the temperature than by the residence time. The mole fraction of oligomers with a molecular weight higher than 1000 Da produced at 260 °C and for a residence time of 90 min is in fact about 0.35, while that obtained at 343 °C for a residence time of 5 min is only 0.075.

An intriguing aspect of this process, which is confirmed both by the experimental investigation as well as by our simulations, is the significant presence of dimers particularly at high temperatures and high residence times. This cannot be justified either by the 1:3 backbiting reaction, for which we calculated a very high activation energy, or by the very slow bimolecular termination between two styrene radicals. However using the developed kinetic model we are now in the position to clarify this issue. In particular, two different pathways have been investigated. First, it has been observed that styrene dimers can be formed as a result of 1:5 and 1:7 backbiting reactions followed by *β*-scission from growing polystyrene chains composed by four and five styrene units, respectively. The abundance of these species is confirmed by experimental observations[10] that show how the molecular weight distribution, in the considered temperature range, is centered about oligomers containing three to six styrene units.

The second investigated mechanism proceeds through the formation of a midchain radical in position 7. This chemical species can further react following three different pathways to give: a radical in position 1 through a backward 7:1 backbiting

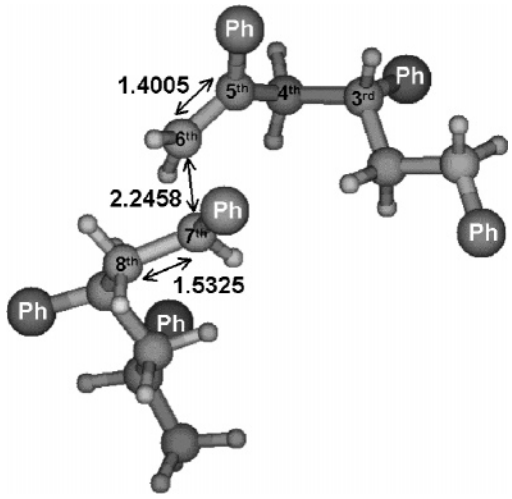

Figure 8. Transition state geometry for the β-scission reaction of the polystyrene radical in position 5 (isotactic molecular model). Distances are reported in angstroms.

Table 6. Rate Constants for β-Scission and Termination Reactions Calculated Using the Isotactic Model[a]

reaction		$\log_{10} A$	E_a
$S \rightarrow R_{1,1}$	k_I	8.276	27.44
$R_{n,1} + S \rightarrow R_{n+1,1}$	k_{cp}	10.137	8.43
$R_{n+1,1} \rightarrow R_{n,1} + S$	k_{cp}^{-1}	9.748	19.57
$R_{n,3} \rightarrow P_2 + R_{n-2,1}$	$k_{\beta 3}^{right}$	12.707	20.63
$R_{n,3} \rightarrow P_{n-1} + R_{1,1}$	$k_{\beta 3}^{left}$	12.719	22.50
$R_{n,5} \rightarrow P_3 + R_{n-3,1}$	$k_{\beta 5}^{right}$	12.737	20.00
$R_{n,5} \rightarrow P_{n-2} + R_{2,1}$	$k_{\beta 5}^{left}$	12.737	20.00
$R_{n,7} \rightarrow P_4 + R_{n-4,1}$	$k_{\beta 7}^{right}$	12.487	24.02
$R_{n,7} \rightarrow P_{n-3} + R_{3,1}$	$k_{\beta 7}^{left}$	12.487	24.02
$R_{n,1} + R_{m,1} \rightarrow P_{n+m}$	k_{ta}	12.050	0.0
$R_{n,1} + R_{m,1} \rightarrow P_n + P_m$	k_{td}	11.180	1.50

[a] Left and right rate constants were assumed to be the same for the β5 and β7 scission reactions. Pre-exponential factors and activation energies were reported in units consistent with kcal, s, mol, and cm as $k = A \exp(-E_a/RT)$. Experimental values of initiation[1] (k_I) and termination by disproportionation[34] (k_{td}) are included and have been used in the reactor simulations.

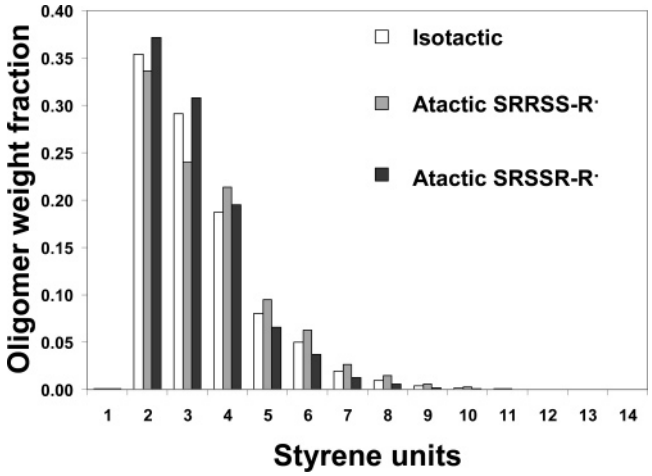

Figure 9. Molecular weight distribution calculated at 343 °C for 90 min residence time using three different kinetic schemes.

reaction, a radical in position 3 through a 7:3 backbiting reaction or a dead chain and a radical through a β-scission reaction. As discussed above the rate of the 7:3 backbiting reaction is similar to that of the 1:5 reaction. The 7:1 backward reaction is the slowest while the β-scission is only slightly faster than the 7:3

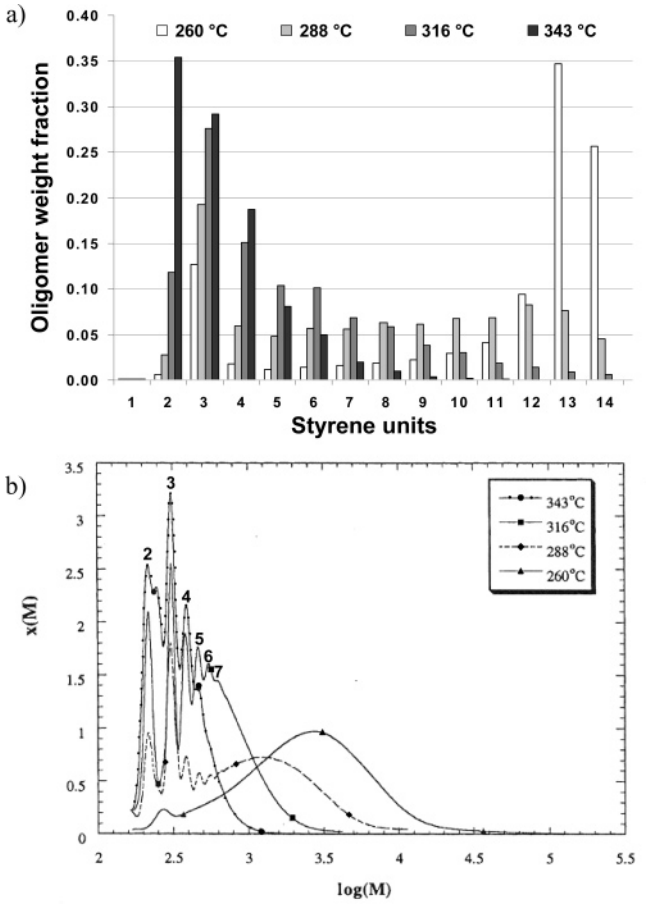

Figure 10. (a) Molecular weight distribution obtained for 90 min residence time at different temperatures: 260, 288, 316, and 343 °C (isotactic kinetic scheme). (b) Experimental results taken from ref 10; the number of styrene units of the first peaks is reported to help the comparison with the calculated data.

backbiting reaction. Thus, this appears as a feasible reaction pathway for the production of a radical in position 3. After being generated, the radical in position 3 can then react following pathways similar to those previously described for the radical in position 7. This chemical pathway, characterized by a succession of β-scission and backbiting reactions, is sketched in Scheme 4, while the values of the corresponding rate constants are reported in Table 5 and 6.

As it can be observed, this kinetic mechanism provides a pathway for the formation of dimers that does not require passing through a 1:3 backbiting reaction or a bimolecular termination by combination. To test the importance of the contribution of this reaction pathway to the formation of dimers, some simulations were made changing systematically the global kinetic mechanism. First, simulations were performed suppressing the 1:3 backbiting reactions, which lead to a substantially unchanged polymer weight distribution and thus confirmed the irrelevance of this mechanism. On the other hand the elimination of the 7:3 backbiting reactions (and of the corresponding backward reactions) produces at 343 °C a polymer weight distribution with a reduction of about 20% of dimers concentration. Similarly, simulations performed without considering β-scission reactions of growing radicals formed by four or five monomers led to a decrease of about 15% of the amount of dimers in the final products. Thus, it can be concluded that the two pathways proposed to explain the dimer production mechanism play both an important role in the high-temperature styrene polymerization.

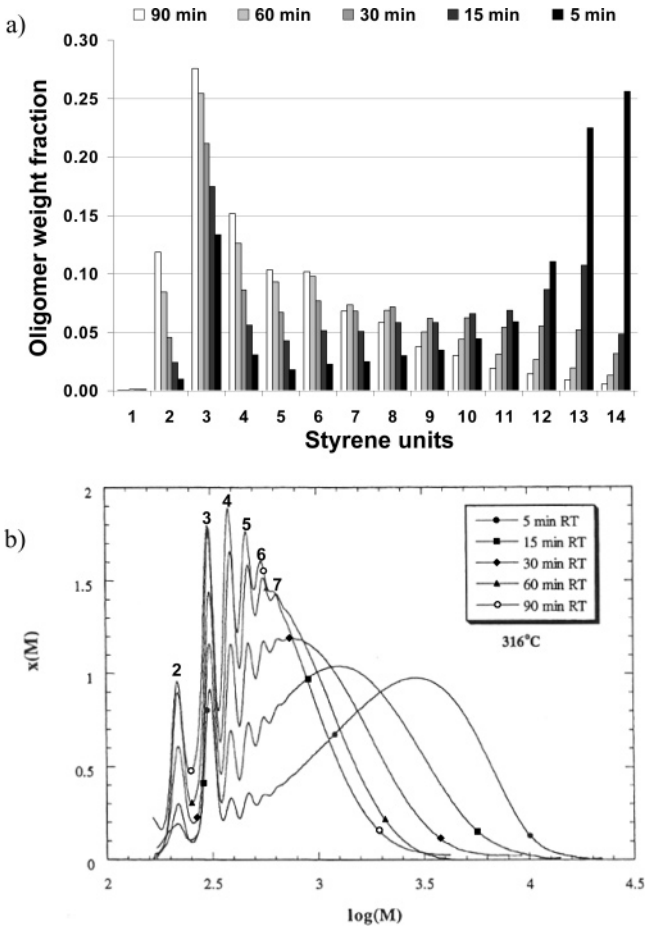

Figure 11. (a) Molecular weight distribution calculated at 316 °C and five residence times: 5, 15, 30, 60, and 90 min (isotactic kinetic scheme). (b) Experimental results taken from ref 10; the number of styrene units of the first peaks is reported to help the comparison with the calculated data.

Scheme 4. Second Chemical Pathway Proposed for the Formation of Styrene Dimers from Right β-scission Reactions

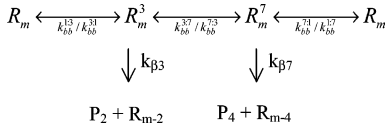

It is interesting to note that the two new chemical pathways investigated above lead to the production of dimers with a slightly different chemical structure. In particular, as shown in Scheme 5, the product of the first investigated mechanism is the 2,4-diphenyl-1-pentene, while the second one leads to 2,4-diphenyl-1-butene. Although these are both "dimers", they have a molecular weight which differs by about 10%: 222 Da and 208, which in terms of log(*M*) correspond to 2.35 and 2.32, respectively. By a close inspection of the experimental results at 343 °C and 90 min residence time (Figure 10b), it can be clearly seen that in the proximity of the dimer molecular weight two different peaks are present. This peak splitting has never been discussed in previous papers, but using our computational results, it can be explained through the existence of two equivalent pathways that produce different "dimers". In order to further confirm the above result, one can now investigate with the model why the splitting of the dimer peak occurs only at 343 °C while it disappears at lower temperatures. This can be explained by considering the effect of temperature on the rates of the different reactions that control the chain termination

Scheme 5. Reactions That Can Lead to the Production of Styrene Dimers

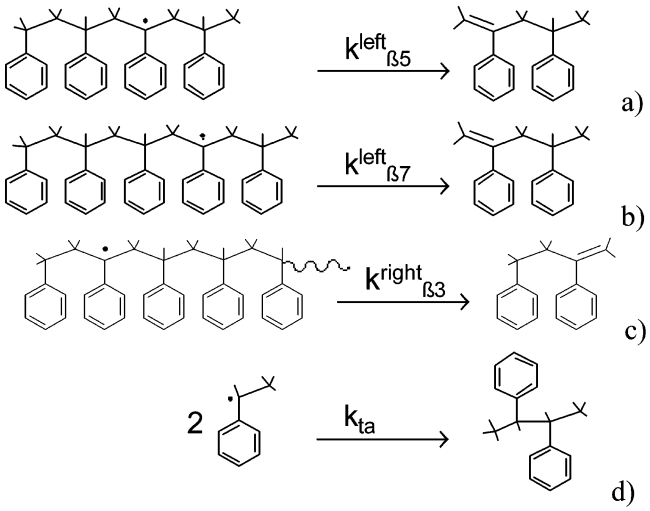

process. Simulations performed at lower temperatures, in fact, show a decrease of the production of 2,4-diphenyl-1-pentene while bimolecular termination reactions (in particular termination by combination) become more important, as discussed in detail in the following.

In agreement with the conclusion of Campbell et al.,[10] the developed kinetic model shows that the dominant chain termination mechanism proceeds through monomolecular rather than bimolecular reactions. This can be clearly seen by comparing the relative contribution of the two mechanisms to the formation of oligomers as predicted by the reactor model based on the global kinetic mechanism. The results are shown in Figure 12 for different temperatures and residence times. The mole fraction of each oligomer is reported in ordinates, while the uniform and dashed areas represent the contribution of bimolecular and monomolecular terminations, respectively. Monomolecular dominates over bimolecular termination reactions for all the considered operating conditions. Note that the contribution of bimolecular terminations depends on the produced oligomer length, and it is most important for oligomers having a molecular weight comprised between 500 and 1000 Da, which are however present in a very low concentration. A comparison of the results in Figure 12, parts a and b, shows that the relative contribution of monomolecular and bimolecular reactions to the formation of the various oligomers is almost independent of temperature and residence time, except for the dimers, for which the temperature decrease from 343 to 288 °C leads to a corresponding decrease of the monomolecular contribution from 94.9% to 78%. Finally, it is worth noting that by comparing the rates of the two bimolecular termination reactions it appears that combination is favored upon disproportionation. The chemical structure of the dimer produced through combination by reaction d of Scheme 5, 2,3-diphenylbutane, is very close to that of 2,4-diphenyl-1-butene (210 vs 208 Da), which is produced by disproportionation. This is coherent with the absence of the splitting of the dimer peaks at temperatures lower than 343 °C.

Summarizing, it can be concluded that the high-temperature styrene polymerization is a complex process that is not characterized by a single rate-determining step. Although monomolecular termination reactions dominate over bimolecular reactions, the termination process is characterized by a succession of backbiting and β-scission reactions that have similar rates. Thus, with reference to Scheme 1, the rate of

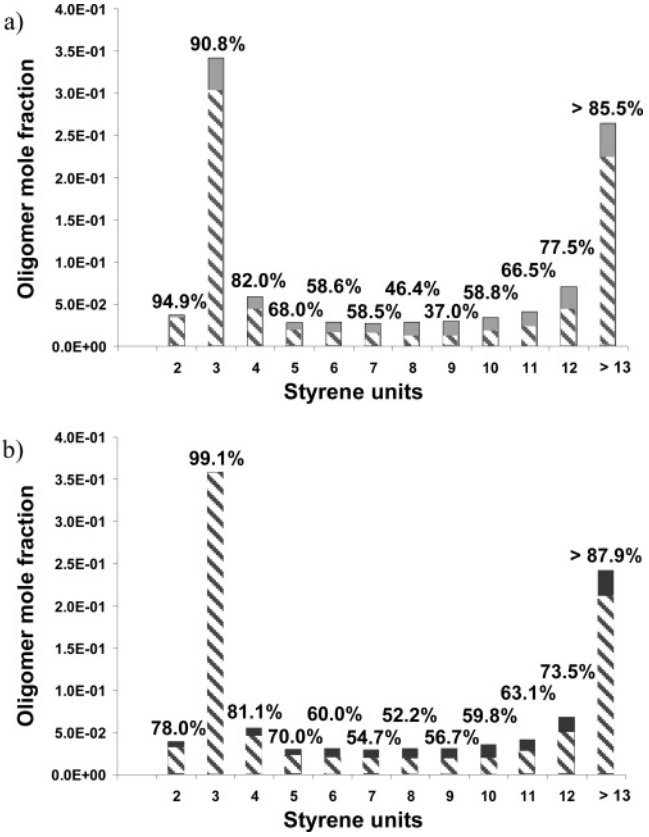

Figure 12. Contributions in terms of oligomers production of monomolecular (dashed area and number are the percentage of produced oligomer) and bimolecular termination reactions in simulations performed at different temperatures and residence times: (a) oligomers produced at 343 °C with a residence time of 5 min; (b) oligomers produced at 288 °C with a residence time of 30 min (isotactic kinetic scheme).

production of a mid chain radical is similar to the rate of both its backbiting reactions, which lead to the transfer of the radical on a different position along the chain, and its β-scission decomposition.

4. Conclusions

The subject of this work has been the computational investigation of the high-temperature polymerization of styrene. The most important kinetic constants involved in the process have been calculated using classic and variational transition state theory on PES determined with a hybrid approach. Following a multiscale strategy[41,42] aimed at verifying the consistence between microscopic rate estimation and macroscopic measurements, the kinetic constants calculated by quantum chemistry have been embedded into a CSTR model and the polymerization process was simulated. The predicted structures of the produced oligomers as a function of the operating conditions, i.e., temperature, pressure, and residence time, are in good agreement with the experimental data.

With respect to previous kinetic models, the global kinetic mechanism developed in this work is characterized by the presence of a new 7:3 backbiting reaction as well as by the explicit consideration of the reversibility of all backbiting reactions. Specific attention has been devoted to the production of styrene dimers. The mechanism proposed in literature to explain the formation of dimers includes the 1:3 backbiting reaction, which we found however to be hindered by a very high activation energy. On the other hand, we found that dimers are produced at high temperature following two different types of monomolecular termination reactions that lead to the production of two different styrene dimers: 2,4-diphenyl-1-pentene and 2,4-diphenyl-1-butene. These results are in accordance with the MALDI−TOF experimental data, which show the presence of two dimers with the corresponding molecular masses. At lower temperatures we found that both mono and bimolecular reactions are active in the production of dimers; in this case the two different products (2,4-diphenyl-1-butene and 2,3-diphenylbutane) are not experimentally distinguishable.

Notation

k_{af}	addition fragmentation rate constant
k_{bb}	backbiting rate constant
k_{ctp}	chain transfer to polymer rate constant
k_{cp}	propagation rate constant
k_{tc}	termination rate constant by combination
k_{td}	termination rate constant by disproportionation
k_{β}	β-scission rate constant
P_n	dead polymer chain of length n
R_n	radical chain of length n
$R_{n,m}$	radical chain of length n with radical in m position
S	styrene

Supporting Information Available: Tables of geometries of reactants, products, and transition states and figures showing molecular weight distributions calculated for the two atactic chain kinetic schemes considered. This material is available free of charge via the Internet at http://pubs.acs.org.

References and Notes

(1) Hui, A. W.; Hamielec, A. E. *J. Appl. Polym. Sci.* **1972**, *16*, 749.
(2) Husain, A.; Hamielec, A. E. *J. Appl. Polym. Sci.* **1978**, *22*, 1207.
(3) Hamielec, A. E.; MacGregor, J. F. *Polymer Reaction Engineering*; Reichert, K. H., Geisler, W., Ed.; Huting and Wepf: New York, 1986.
(4) Kirchner, K.; Katzenmayer, T. *Polymer Reaction Engineering*; Geisler, W., Ed.; Huting and Wepf: New York, 1986.
(5) Woo, O. S.; Broadbelt, L. *Catal. Today* **1998**, *40*, 121.
(6) Wang, M.; Smith, J. M.; McCoy, B. *AIChE* **1995**, *41*, 1521.
(7) Spychaj, T.; Hamielec, A. E. *J. Appl. Polym. Sci.* **1991**, *42*, 2111.
(8) Madras, G.; Smith, J. M.; McCoy, B. *J. Ind. Eng. Chem. Res.* **1996**, *35*, 1795.
(9) Mayo, F. R. *J. Am. Chem. Soc.* **1968**, *90*, 1289−1295.
(10) Campbell, J. D.; Teymour, F.; Morbidelli, M. *Macromolecules* **2003**, *36*, 5491−5501.
(11) Campbell, J. D.; Ph.D. Thesis, Swiss Federal Institute of Technology: Zurich, Switzerland, 2003.
(12) Fascella, S.; Cavallotti, C.; Rota, R.; Carrà, S. *J. Phys. Chem. A* **2004**, *108*, 3829−3843.
(13) Fascella, S.; Cavallotti, C.; Rota, R.; Carrà, S. *J. Phys. Chem. A* **2005**, *109*, 7546−7557.
(14) Cavallotti, C.; Moscatelli, D.; Carrà, S. *J. Phys. Chem. A* **2004**, *108*, 1214−1223.
(15) Deng, L.; Woo, T. K.; Cavallo, L.; Margl, P. M.; Ziegler, T. *J. Am. Chem. Soc.* **1997**, *19*, 6177−6186.
(16) Deng, L.; Margl, P.; Ziegler, T. *J. Am. Chem. Soc.* **1999**, *121*, 6479−6487.
(17) Woo, T. K.; Margl, P. M.; Deng, L.; Cavallo, L.; Ziegler, T. *Catal. Today* **1999**, *50*, 479−500.
(18) Guerra, G.; Longo, P.; Corradini, P.; Cavallo, L. *J. Am. Chem. Soc.* **1999**, *121*, 8651−8652.
(19) Woo, T. K.; Patchkovskii, S.; Ziegler, T. *Comput. Sci. Eng.* **2000**, 28−37.
(20) Milano, G.; Guerra, G.; C.; P.; Cavallo, L. *Organometallics* **2000**, *19*, 1343−1349.
(21) Maseras, F.; Morokuma, K. *J. Comput. Chem.* **1995**, *16*, 1170−1179.
(22) Vreven, T.; Morokuma, K. *J. Comput. Chem.* **2000**, *21*, 1419−1432.
(23) Stewart, J. J. P. *J. Comput. Chem.* **1989**, *10*.
(24) Hohenberg, P.; Kohn, W. *Phys. Rev.* **1964**, *136*, B864.
(25) Kohn, W.; Sham, L. J. *Phys. Rev.* **1965**, *140*, A1133.
(26) Becke, A. D. *J. Chem. Phys.* **1993**, *98*, 5648−5652.
(27) Lee, C.; Yang, W.; Parr, R. G. *Phys. Rev. B* **1988**, *37*, 785−789.
(28) Dunning, T. H., Jr.; Hay, P. J. *Modern Theor. Chem.* **1976**, *3*, 1.

(29) Van Speybroeck, V.; Van Neck, D.; Waroquier, M.; Wauters, S.; Saeys, M.; Marin, G. B. *J. Phys. Chem. A* **2000**, *104*, 10939−10950.
(30) Peng, C.; Ayala, P. Y.; Schlegel, H. B.; Frisch, M. J. *J. Comput. Chem.* **1996**, *17*, 49.
(31) Frisch, M. J. *Gaussian 03, Revision C. 02*; Gaussian: Wallingford CT, 2004.
(32) Schaftenaar, G.; Noordik, J. H. *J. Comput.-Aided Mol. Design* **2000**, *14*, 123−134.
(33) Buback, M.; Gilbert, R. G.; Hutchinson, R.; Kumperman, B.; Kutcha, F. D.; Manderes, B. B.; O'Driscoll, K. F.; Russel, G.; Schweer, J. *J. Macromol. Chem. Phys.* **1995**, *196*, 3267.
(34) Buback, M.; Kutcha, F. D. *J. Macromol. Chem. Phys.* **1997**, *198*, 1455.
(35) *Handbook of Chemistry and Physics*; CRC Press: Boca Raton, FL, 2003−2004.
(36) Gilbert, R. G.; Smith, S. C. *Theory of Unimolecular and Recombination Reaction*; Blackwell Scientific Publication: Oxford, England, 1990.
(37) Gilbert, R. G.; Smith, S. C.; Jordan, M. J. T.; UNIMOL program suite, 1993.
(38) Curran, H. J.; Gaffuri, P.; Pitz, W. J.; Westbrook, C. K. *Combust. Flame* **1998**, *114*, 149−177.
(39) Yamauchi, N.; Miyoshi, A.; Kosaka, K.; Koshi, M.; Matsui, N. *J. Phys. Chem. A* **1999**, *103*, 2723−2733.
(40) Campbell, J. D.; Teymour, F.; Morbidelli, M. *Macromolecules* **2003**, *36*, 5502−5515.
(41) Cavallotti, C.; Di Stanislao, M.; Moscatelli, D.; Veneroni, A. *Electrochim. Acta* **2005**, *50*, 4566−4575.
(42) Cavallotti, C.; Moscatelli, D.; Veneroni, A. *International Series of Numerical Mathematics*: Birkhauser Verlag: Basel/Switzerland, 2005; Vol. 149, pp 29−39.

MA061291K